Chapter 5

Indoor Experimental Characterisation of a Three Trough 50° Effective Acceptance Half-Angle Line-Axis Concentrating Asymmetric Compound Parabolic Photovoltaic Concentrator Using a Continuous Solar Simulator

5.1 Introduction

For photovoltaic applications power output is directly proportional to the incident solar radiation intensity. Increasing the incident radiation level using concentration effectively increases the power output from the photovoltaic, decreasing the production cost of electricity and thus the energy pay back time if both the manufacturing cost and embodied energy is comparative with the standard non-concentrating system. Extensive indoor experimental characterisation of a three trough ACPPVC-50 was undertaken for a wide range of incident solar radiation intensities using a continuous solar simulator.

5.2 Pulsed or Continuous Solar Simulation?

A solar simulator is a device that should produce a spectrum similar to that of the solar spectrum. The solar intensity and other ambient conditions vary continuously in outdoor conditions and are non-controllable, it is therefore difficult to determine cause and effect when a PV system is tested under outdoor conditions. An indoor solar simulator allows the applied conditions to be controllable and therefore cause and effect are identifiable clearly. Major concerns in the design of a solar simulator are the spectral intensity, angular distribution and the uniformity of the illuminated area. Solar simulators detailed in the literature use a multi-stage re-imaging process before the radiation is incident on the test system (Bennett and Podlesny, 1990; Kuhn and Hunt, 1991; Nagamine et al., 1993; Kilmer, 1994; Thomas et al., 2000). Solar simulators may be categorised as

(i) Pulsed, or

(ii) Continuous.

Pulsed simulators provide a desired intensity within in a very short period of time, generally in the order of 1ms. Because the flash from the light source is for a short period of time, the power consumption of this type of simulator is less compared to a continuous simulator. The major advantages of the pulsed simulator are:

- a good spectral match to insolation can be obtained (Nagamine et al., 1993)
- a low mean power consumption due to the short duration of the flash
- ±1% uniformity can be achieved using flash xenon arc lamps over a 0.2 m × 0.2 m illuminated area (Thomas et al., 2000)
- the heating effect on the test system is low.

The major disadvantages of pulsed simulators are:

- data has to be acquired in a very short period of time, less than the flash duration (Sheila et al., 1997)
- the PV system has to have a fast response
- temperature effects on PV system performance cannot be investigated.

A continuous solar simulator provides a constant illumination on the test area for the desired period of time. This type of simulator is suitable for slow response solar cells and has several advantages:

- the measurement equipment required to determine the output voltage and current is less sophisticated (Nagamine et al., 1993)
- temperature effects on the PV system can be investigated
- using custom software dark I-V measurements may be undertaken to determine series resistance, shunt resistance, and diode parameters (Thomas et al., 2000)
- the module I-V characteristics can be determined over an extended range, under reverse or forward bias conditions (Thomas et al., 2000)
- with suitable collimation PV systems can be characterised for a wide range of solar incidence angles.

5.2.1 Continuous Solar Simulator Lamp Selection

For the asymmetric compound parabolic photovoltaic concentrator designed for indoor experimental characterisation a minimum illuminated area of 400 mm × 300 mm is required. Three types of light sources were considered, a single long arc lamp, an array of compact iodide daylight (CID) lamps and stage lighting equipment using high colour temperature high intensity discharge (HID) lamps.

Figure 5.2.1.1 shows the continuous solar simulator used for the indoor experimental characterisation analysis of a three trough ACPPVC-50. The manufacturer's lamp spectrum indicates that the use of OSRAM HMI lamps or Philips MSR lamps is most suitable for solar simulation (Anon, 2001i). These lamps are available in the range from 125 to 4000 W and can provide insolation levels up to 1000 Wm^{-2} over the test area with a colour temperature of between 5000 and 6000 K. Follow spot units used for theatre lighting have an adjustable lens to vary the focal distance of the lamp and can be used to provide the necessary compromise between collimation, uniformity and intensity. Such units also include external filter holders and allow suitable spectral filters to be included for fine adjustment of the spectrum. Such systems allow the area of illumination to be increased in a modular way by the addition of more units with a suitable iris and barn doors.

The solar simulator used in this work had the following features: a 1200W halogen lamp, a zoom optical system, a high light output and uniform focusing, a cooling fan and iris diaphragm. OSRAM HMI lamps are used in this simulator. These lamps are AC-operated discharge lamps in which the luminous arc burns in a dense vapour atmosphere comprising mercury and rare earth halides. The main benefits are (Anon, 2001i):

- Very high luminous efficacy of up to 100 lm/W
- Daylight colour temperature of approximately 6000 K
- High colour rendering index CRI of >90
- Hot restart and dimmable.

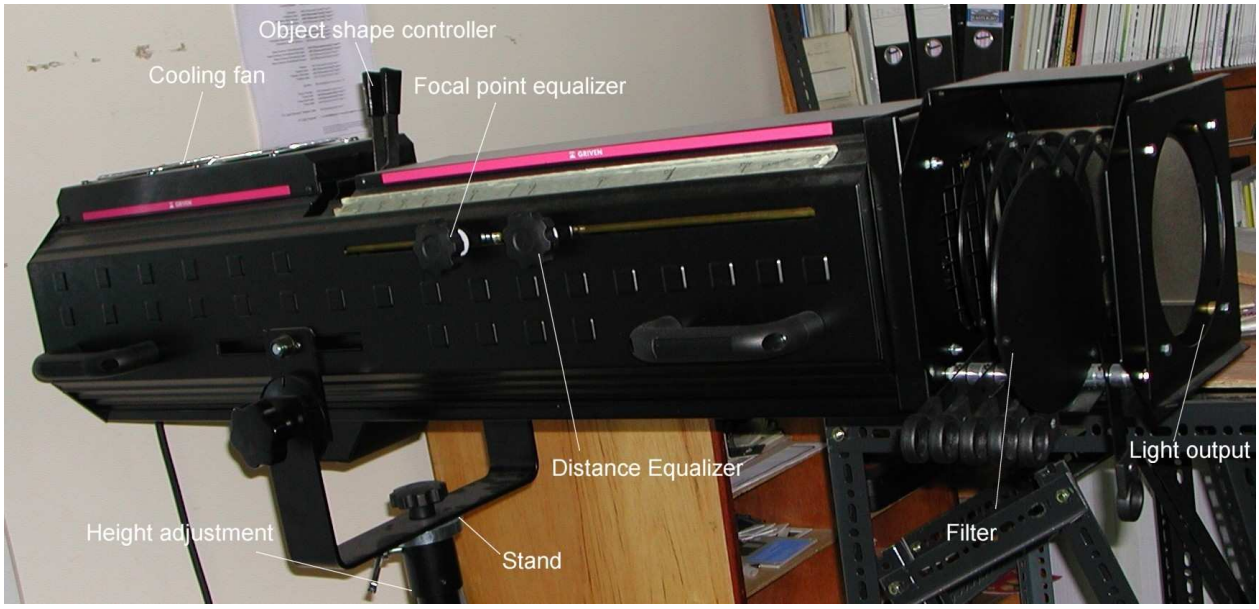

Figure 5.2.1.1 The continuous solar simulator used for the indoor experimental characterisation of the developed asymmetrical compound parabolic photovoltaic concentrator unit.

The lamps illustrated in figure 5.2.1.2 are single-ended with an external bulb that makes the lamps easy to handle and provides optimum noise suppression when operated with electronic control gear. The outer jacket improves the dimming characteristics and allows the lamp to be used in any position. Lamp number 6 in figure 5.2.1.2 was used for this work.

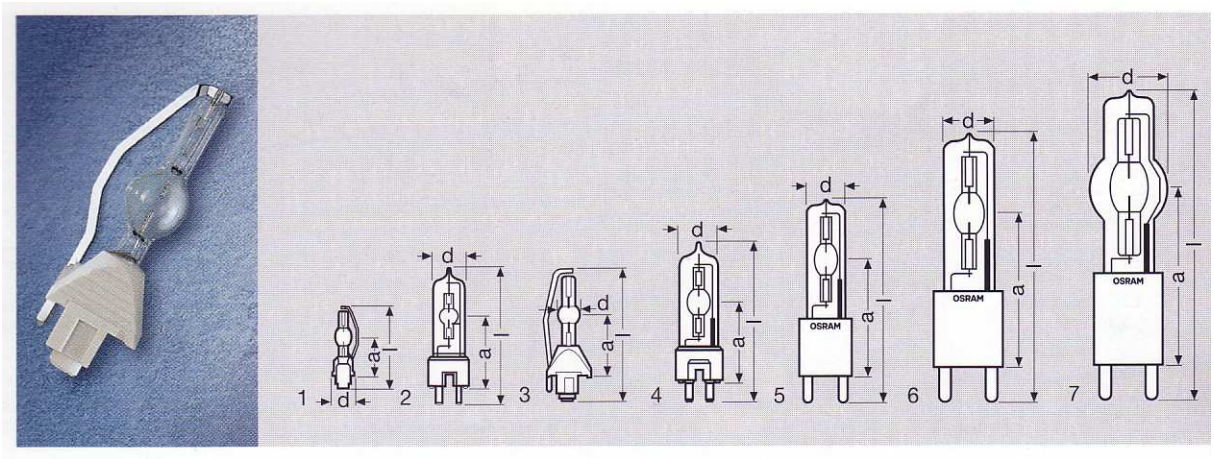

Figure 5.2.1.2 Physical and geometrical characteristics of lamps used in the continuous solar simulator (Anon, 2001i).

For tungsten-halogen lamps a 5% drop in voltage will double the lamp life and reduce the colour temperature as the power decreases (Anon, 2001i). Discharge lamps behave in a similar way for the initial dimming stage with dimming causing a drop in luminous flux. The colour temperature however, increases (i.e. the lamp appears more bluish), while colour rendering deteriorates for the red component in the spectrum. The result is that light from such lamps appears more bluish. These effects can be reduced by regulating the amount of light using grey scale filters or mechanical shutters. The OSRAM HMI lamp continues to operate at full load, so its photometric properties remain more or less constant for every

intensity. If the lamp is dimmed by reducing the voltage it will not reach its optimum operating state and, unlike tungsten-halogen lamps, will have a reduced life span.

The temperature of the bulb wall is lower for a lamp with no outer bulb than on a lamp with an outer bulb in which the discharge tube can only be influenced by the ambient temperatures surrounding the lamp indirectly or at least with a significant time lag. For dimming outer bulb lamps are not as sensitive and a reduction in wattage does not result in significant changes in their colour quality. For these types of lamps forced cooling can reduce, but cannot eliminate temperature-related problems. The in-house solar simulator allowed;

- Characterisation under controlled conditions.
- Comparison of two panels simultaneously under controlled conditions.
- Testing independent of diurnal and seasonal variations.
- Fast and accurate characterisation of panels.
- Temperature effects to be investigated.

Figure 5.2.1.3 shows a schematic diagram of the continuous solar simulator used for the experimental characterisation of the developed ACPPVC-50. The area illuminated by the solar simulator can be adjusted depending on the area of device under test (DUT). The focal length adjustment and illuminated area adjustment screws change the light intensity on the illuminated area. The change in incident flux with the distance from the centre of the illuminated area for differing focal lengths (f1) is shown in figure 5.2.1.4. As expected the flux intensity increases when the illuminated area is reduced. The maximum flux is 400 Wm^{-2} for an area of 0.2m x 0.2m.

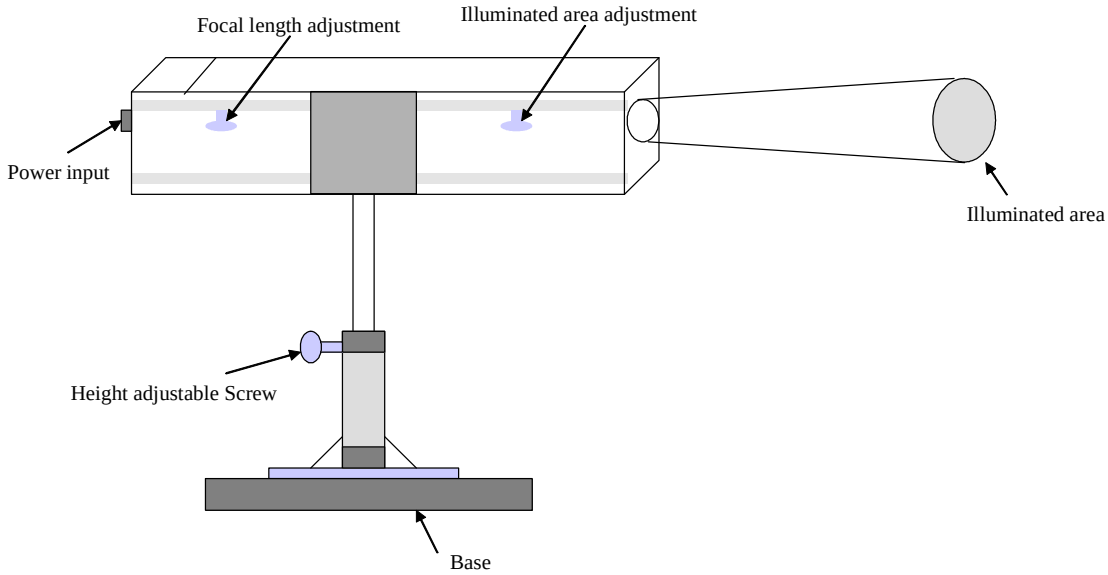

Figure 5.2.1.3 Schematic diagram of the continuous solar simulator.

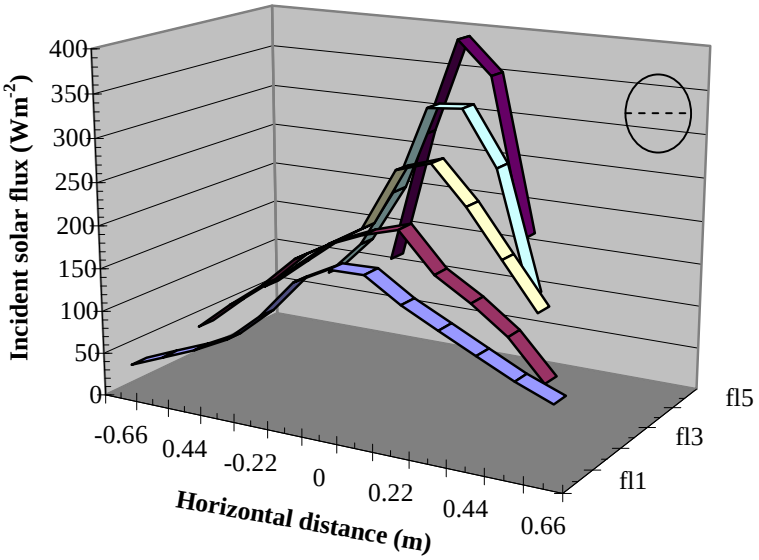

(a)

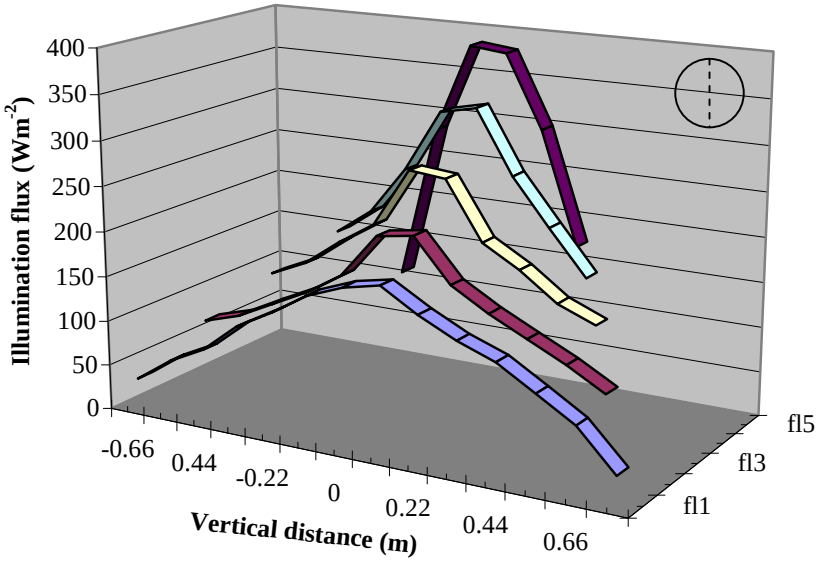

(b)

Figure 5.2.1.4 The incident solar flux intensity for the continuous solar simulator when illuminating different areas (a) horizontally, (b) vertically.

5.2.2 Spectral Characteristics of the Solar Simulator

Figure 5.2.2.1 shows that the spectral distribution for dimmed HMI 1200 lamps used in the simulator. At 100% of rated wattage, the spectral distribution is well matched to the solar spectrum (compare figure 1.4.1 in page 23 and figure 5.2.2.1).

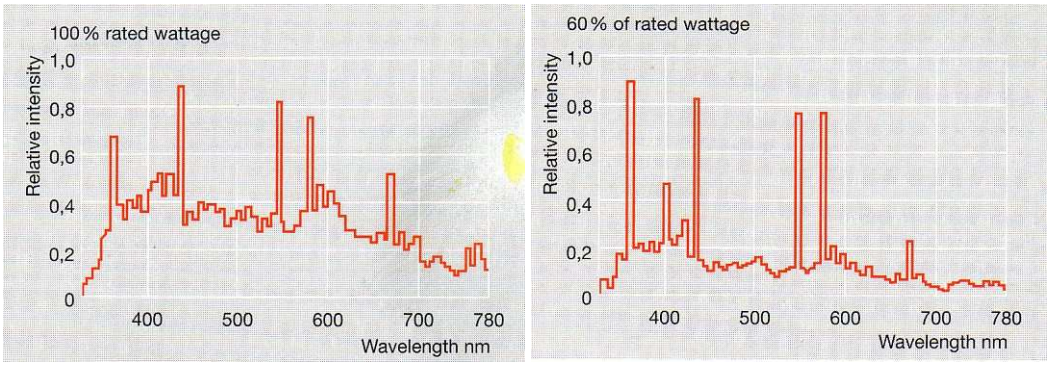

Figure 5.2.2.1 Spectral distributions for HMI 1200 W/GS lamp used in continuous solar simulator for 100% and 60% rated wattage (Anon, 2001i).

5.3 Experimental Set up for the ACPPVC-50 System

Concentrating solar cells operate at greater intensities of solar radiation compared to flat non-concentrating solar PV panels. The current generated from the concentrator panel is linearly proportional to the solar irradiance although the open circuit voltage will change by a small amount. For concentrating systems, the cell temperature will increase decreasing the output power and thus electrical conversion efficiency of the system. The standard measurement circuit for testing a PV panel is shown in figure 5.3.1. This consists of an Ammeter connected in series to measure the current produced by the PV along with a Voltmeter connected in parallel to measure the voltage developed by the photovoltaic when it is illuminated. A variable load (R_L) is connected in parallel across the voltmeter. The variable load changes the internal resistance of the circuit and electrical parameters (voltage and current) being measured.

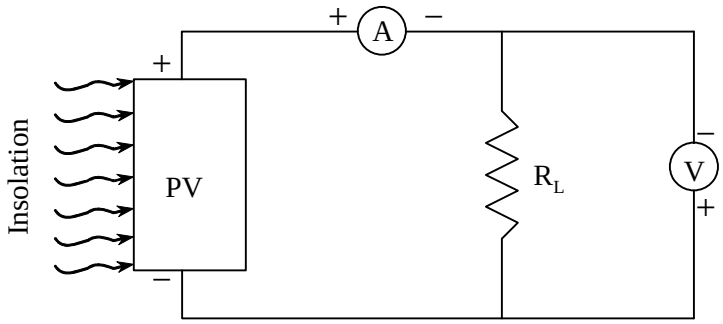

Figure 5.3.1 Standard circuit diagram for I-V curve characterisation of PV system (Komp, 1995).

This simple loading circuit is replaced by an electronic Keithley source meter that performs at a similar desired frequency and accuracy. The circuit diagram showing the equipment used to measure I-V characteristics is shown in figure 5.3.2, a KI2700 data acquisition system measures the current, voltage, temperature, solar insolation and air velocity. The actual values of temperature, solar insolation and wind velocity are computed from the measured voltage, converted by the sensor calibration. The KI2400 source meter is connected with the data acquisition card through an IEEE488 interface to a PC (Koutroulis and Kalaizakis, 2003) on which the data is stored.

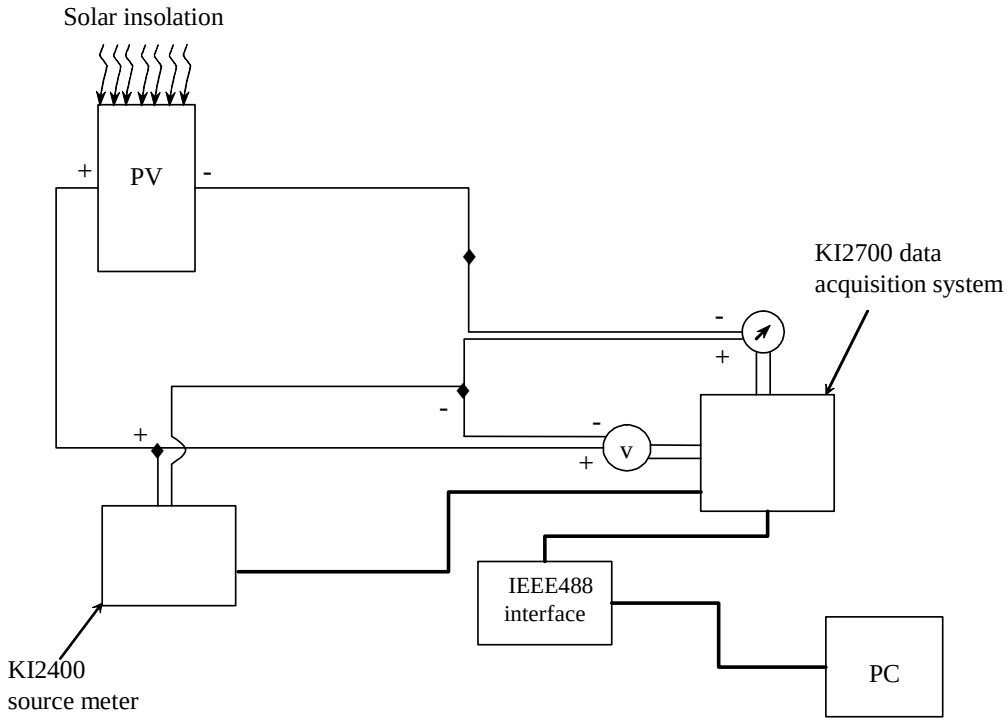

Figure 5.3.2 Modified circuit diagram for continuous I-V measurement of photovoltaic system under illumination conditions.

5.4 Equipment Specification and Sensors Used in the Experiments

Apart from I-V measurements, temperature, solar radiation and wind velocity were measured for the indoor and outdoor experimental characterisation. The equipment specification and sensors used in the experimental characterisation are discussed in Appendix B.

5.5 Indoor Experimental Characterisation of the ACPPVC-50 System

Experiments were performed using a continuous solar simulator to produce the instantaneous voltage and corresponding current along with temperatures and incident radiation. From each set of measured voltage-current data, maximum power point, efficiency and fill factor were determined. Figure 5.5.1 shows the ACPPVC-50 system under test using the solar simulator. The pyranometer measures the solar radiation at each and every set of measurements of output voltage and current. The pyranometer was set off centre for the test cell, a measurements where based upon a datum reference for the cell test area. Figure 5.5.2 shows an enlarged view of the ACPPVC-50 undergoing experimental characterisation. As seen in figure 5.5.1, the output from the ACPPVC-50 is connected directly to the Keithley data acquisition and source meter through the IEEE488 interface linked to a PC. Each complete set of voltage, current, solar radiation and temperature measurements took approximately 10 seconds. For each “single” measurement, 100 readings were taken and averaged, a complete set of I-V measurements therefore corresponds to 8000 readings.

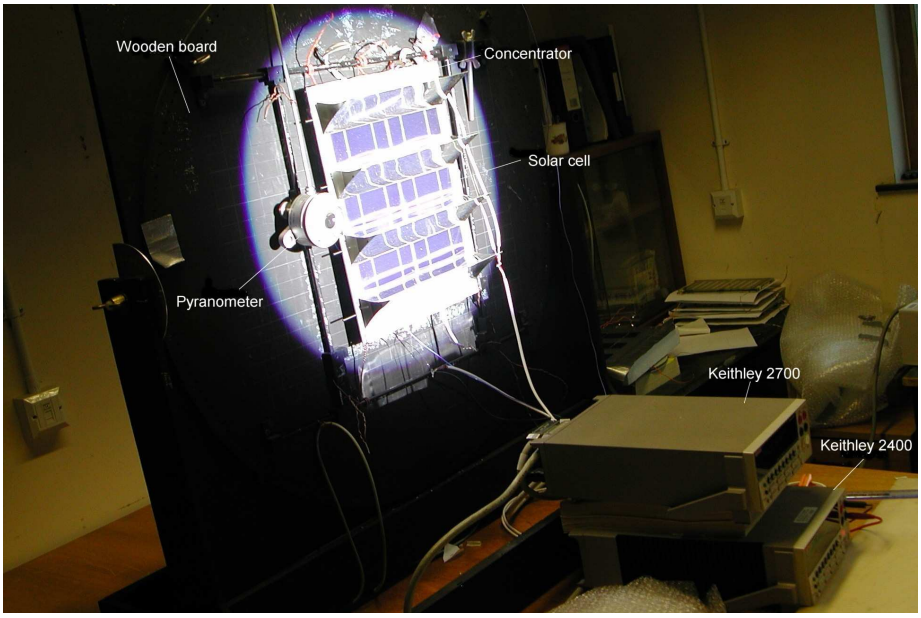

Figure 5.5.1 Experimental characterisation of an ACPPVC-50 using the solar simulator.

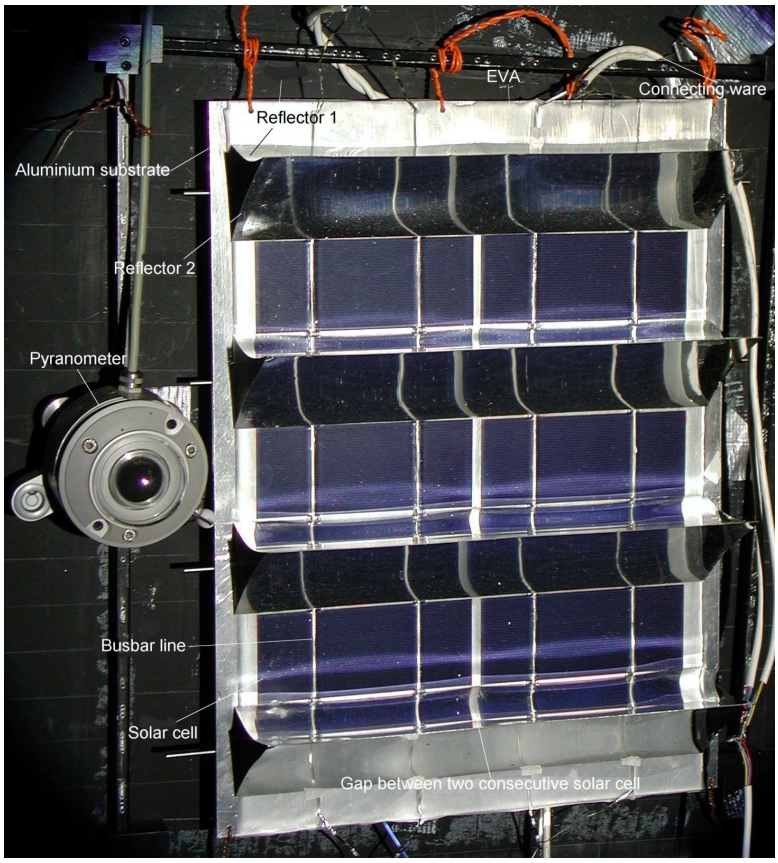

Figure 5.5.2 Enlarged view of the ACPPVC-50 used for indoor experimental characterisation.

The bi-polar source meter can source and measure voltage in both positive and negative directions. A small negative voltage of magnitude -0.2V was applied from the source meter to measure short circuit current accurately for all the measurements. The open circuit voltage was taken by sending a “switch off” command to the source meter while the upper limit of the sweep point was 0.5V higher than to its

approximate open circuit voltage. The sweep voltage was increased by 0.2V increments up to the required voltage level depending on the PV panel voltage. Programming was implemented in "Visual Basic" and "Test Point" (Anon, 2001j) with the driver routines compiled and linked with the main program before execution. For a simple sweep generation by the source meter, a linear sweep was programmed on the source meter output and the corresponding current and voltage data read into the PC through the read channels of the data acquisition system.

The indoor experimental test was carried out for a number of panels as described below:

1. **Panel 1**: a flat non-concentrating panel with three 50-mm wide BP SATURN solar cell (Anon, 2001e) connected in series.
2. **Panel 2**: a concentrating three trough ACPPVC-50 panel with six solar cells (Anon, 2001e) connected in series as described in chapter 3.
3. **Panel 3**: a flat non-concentrating panel with ten 9-mm wide BP SATURN solar cells connected in series (Anon, 2001k).
4. **Panel 4**: a flat non-concentrating solar panel with 25 BP SATURN solar cells of 3-mm width connected in series. (Anon, 2001l).

5.5.1 I-V Characteristics of the ACPPVC-50 System with Different Incident Solar Radiation Intensities

The I-V characteristic of **Panel 1** is shown in figure 5.5.1.1. The measurements were taken over a period of several days. Ambient room temperature was 20ºC, windows and doors were closed to avoid unwanted air flow and temperature variations. The radiation incidence angle was 0º (perpendicular to the PV which was mounted on a wooden board). Figure 5.5.1.1 shows that the current and voltage generated by the panel increases as the solar radiation intensity increases. The rate of current generation increase was significantly larger than that of the voltage as expected from the solar cell characteristic. The short circuit current increased by 78% when solar radiation increased from 150 Wm^{-2} to 300 Wm^{-2}, compared to an increase of 62% when the solar radiation increased from 200 Wm^{-2} to 400 Wm^{-2}. However, as shown in figure 5.5.1.1 the maximum power increased by 100% when the incident solar radiation increased by 100%.

The I-V characteristic of the three trough asymmetric compound parabolic photovoltaic system **Panel 2** is shown in figure 5.5.1.2 for a range of incident radiation intensities. The measurements were taken under the same conditions as for the flat panel. Each complete set of measurements took 10 seconds. Because of the larger size it was not possible to take measurements at higher solar radiation intensities.

The I-V curve for the ACPPVC-50 panel exhibit a similar pattern to that of the flat panel. A 0.72 A short circuit current was measured for a solar radiation intensity of 250 Wm^{-2} for **Panel 2** compared to the 0.42 A short circuit current produced by **Panel 1** at the same insolation level. As expected the open circuit voltage was nearly double that of **Panel 2** since it has six solar cells connected in series. Minimum cable lengths were used for both systems to minimise the resistive power loss in the power cable. This

loss is more significant for **Panel 1** compared to **Panel 2**, this loss can be reduced by having a PV panel which produces higher voltage but lower current.

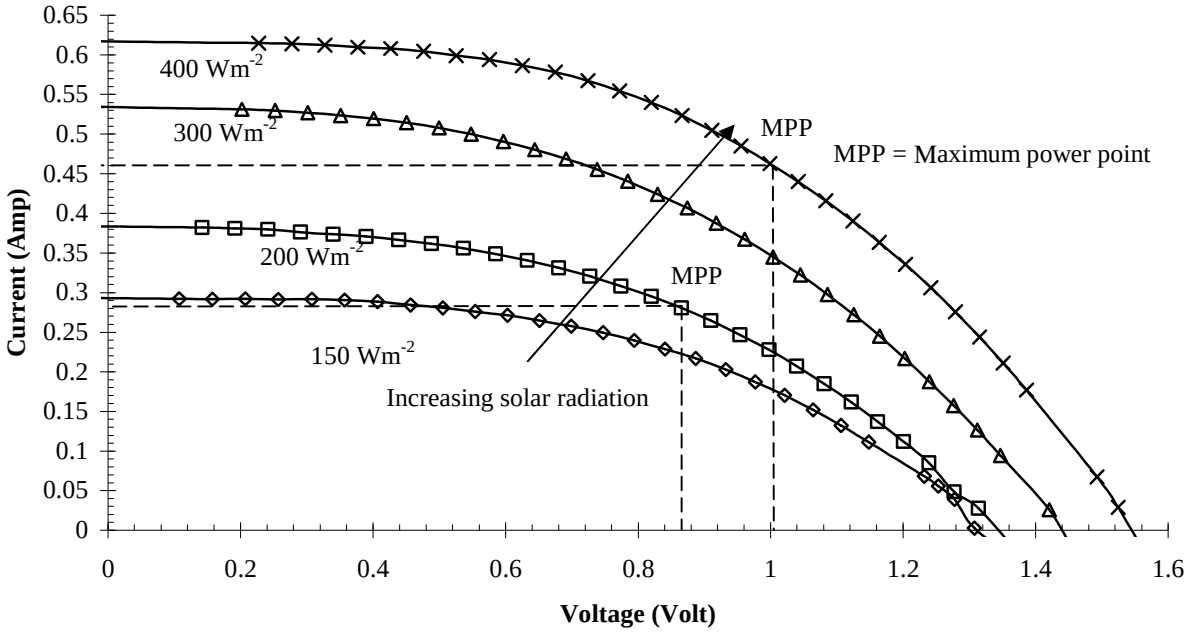

Figure 5.5.1.1 I-V characteristics for a non-concentrating flat panel with three solar cells connected in series for different incident radiation intensities. The ambient room temperature was 20ºC for all measurements and the solar incidence angle was 0º.

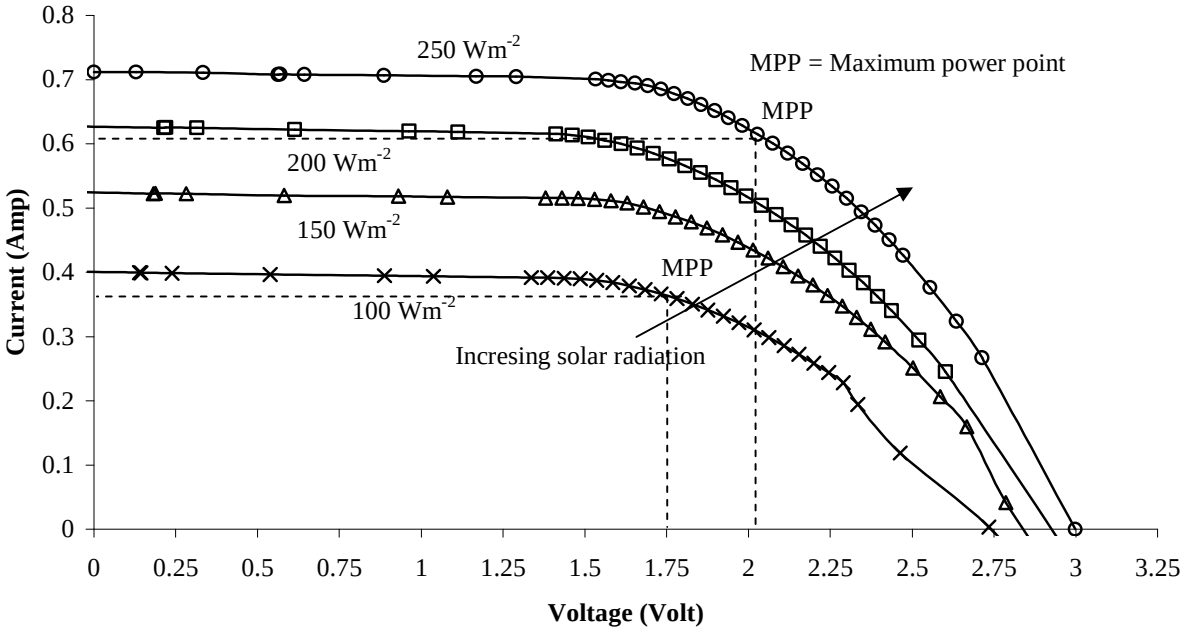

Figure 5.5.1.2 I-V characteristics of the ACPPVC-50 for different incident radiation intensities. The ambient room temperature was 20ºC for all measurements and the solar incidence angle was 0º.

Figure 5.5.1.3 shows the measured I-V curves for **Panel 1** and **Panel 2** for incident radiation intensity of 250 Wm^{-2}. Both panels use the same type of solar cells but because double the number of solar cells are connected in series in **Panel 2** compared to **Panel 1,** the open circuit voltage is nearly doubled.

For **Panel 1** the ideal maximum power ($I_{sc} \times V_{oc}$) is 0.615 W where as for the concentrating **Panel 2** it becomes 2.41 W.

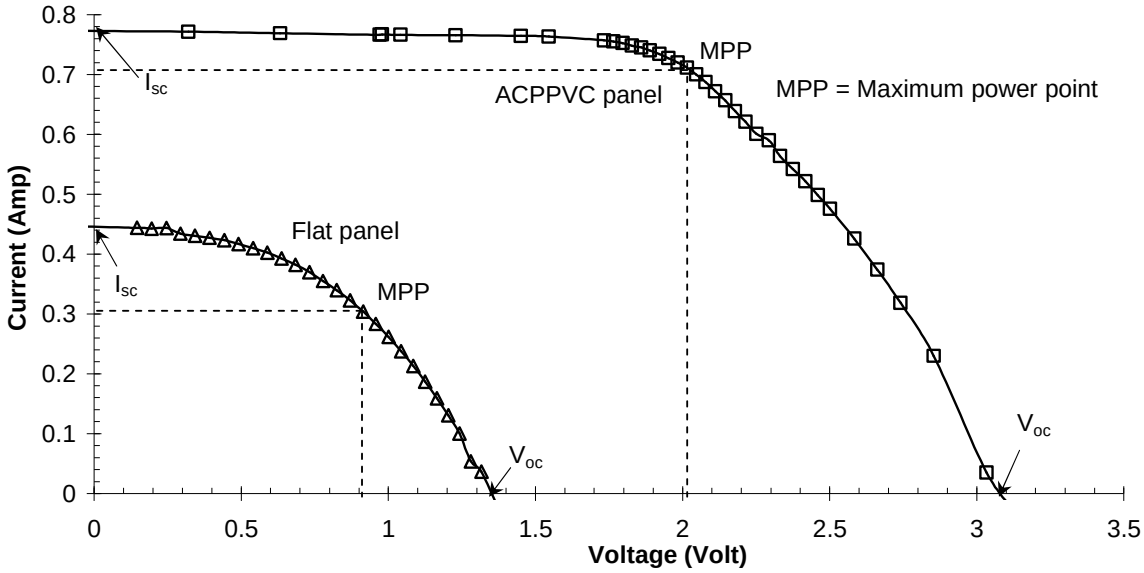

Figure 5.5.1.3 I-V characteristics for flat non-concentrating panel and the ACPPVC-50 for incident radiation intensity of 250 Wm^{-2}. Room temperature was 20ºC for all the measurements and the radiation incidence angle was 0º.

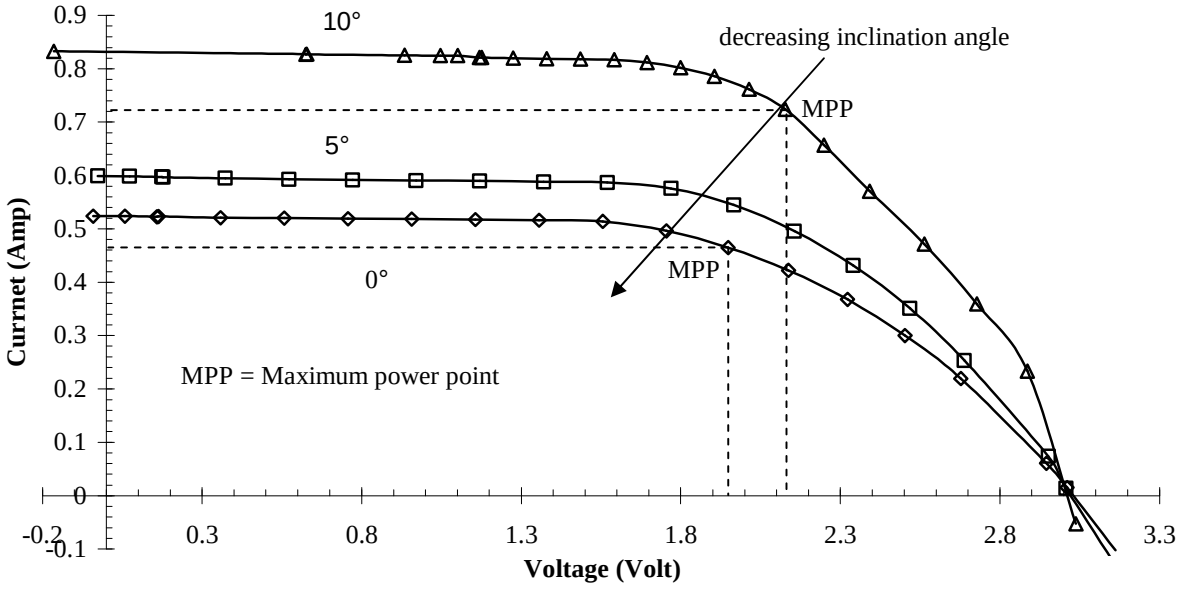

Figure 5.5.1.4 I-V characteristics for the ACPPVC-50 for inclination angles of 0, 5 and 10°. The ambient temperature was 20ºC for all the measurements and the radiation incidence angle was perpendicular to the wooden mounting stand.

As detailed in chapter 2, 100% collection efficiency is predicted for a wide range of solar incidence angles for the ACPPVC-50 system. The I-V characteristics for the ACPPVC-50 are shown in figure 5.5.1.4 for three different inclination angles. The incident radiation intensity was 250 Wm^{-2} perpendicular to the wooden mounting board. As seen in figure 5.5.1.4, the short circuit current increased by 59% when the inclination angle changed from 0° to 10º. This is because at 10º inclination angle 100% collection efficiency is achieved and the predicted optical efficiency at this inclination angle achieves its highest value of 85.25% as detailed in chapter 2.

Laboratory experiments were undertaken for three flat panels (**Panel 1**, **Panel 3** and **Panel 4**) under identical conditions using a switching relay card. The panel configurations along with the data acquisition system and source meter are shown in figure 5.5.1.5. Each full set of measurements of current, voltage, solar radiation and temperatures took approximately 30 seconds to complete for all the three panels. A 5 second time interval was required to reset the instrument for intermediate measurements.

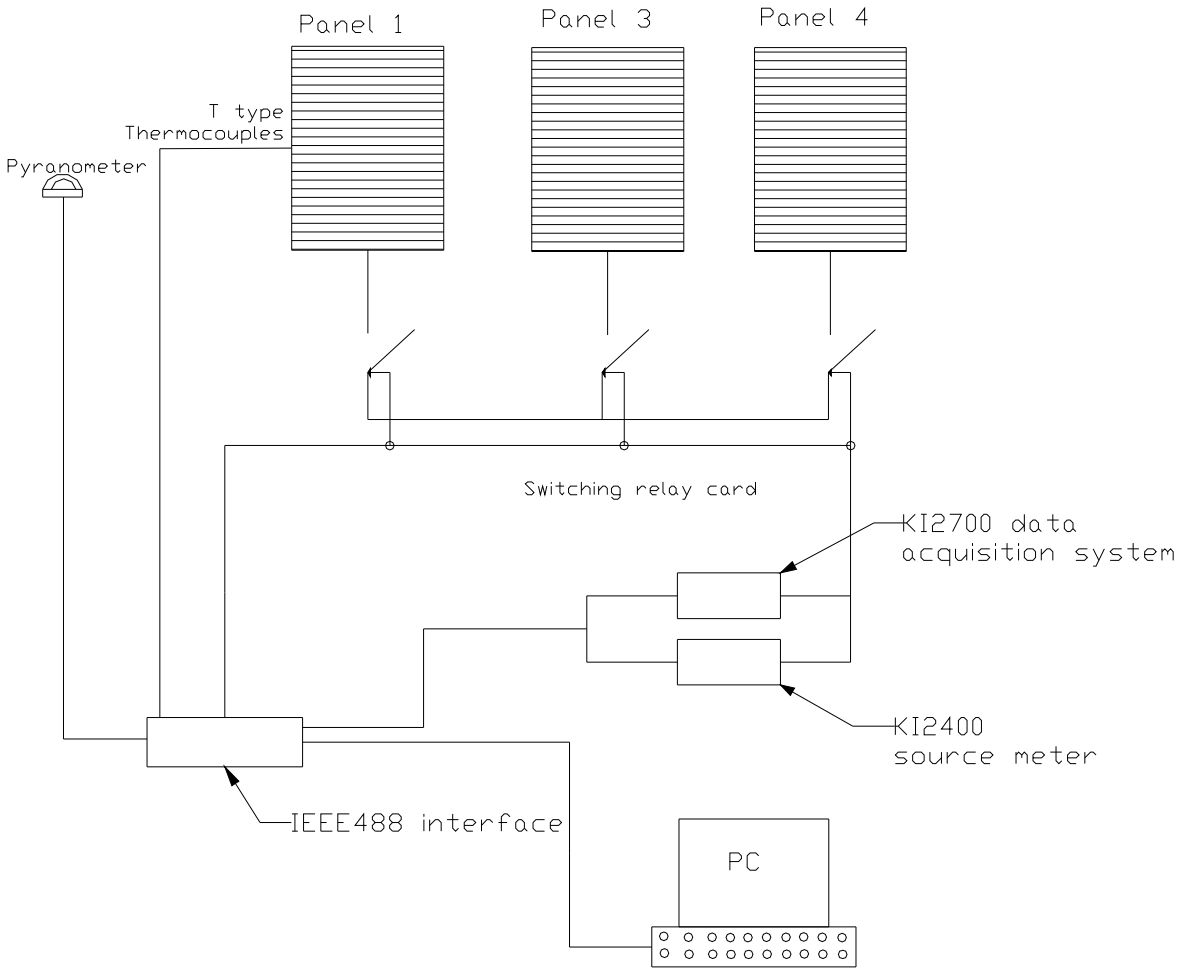

Figure 5.5.1.5 Indoor experimental characterisation of three flat non-concentrating PV panels using a relay switching card.

The I-V characteristic of **Panel 1** with 50-mm wide solar cells is shown in figure 5.5.1.6 for an incident radiation intensity of 200 Wm^{-2}. Figure 5.5.1.7 and figure 5.5.1.8 show the I-V characteristics of **Panel 3** and **Panel 4** for the same solar radiation intensity. The short circuit current is as expected higher for **Panel 1** compared to **Panel 3** and **Panel 4**. This is because the effective solar cell area for **Panel 1** is 0.01875 m^2 compared to 0.009 m^2 and 0.00825 m^2 for **Panel 3** and **Panel 4** respectively. The short circuit current to open circuit voltage ratio for **Panel 3** and **Panel 4** are 0.008 and 0.0016 AV^{-1} compared to 0.266 AV^{-1} of **Panel 1** and therefore the power loss is more significant for **Panel 1** compared to **Panel 3** and **Panel 4**.

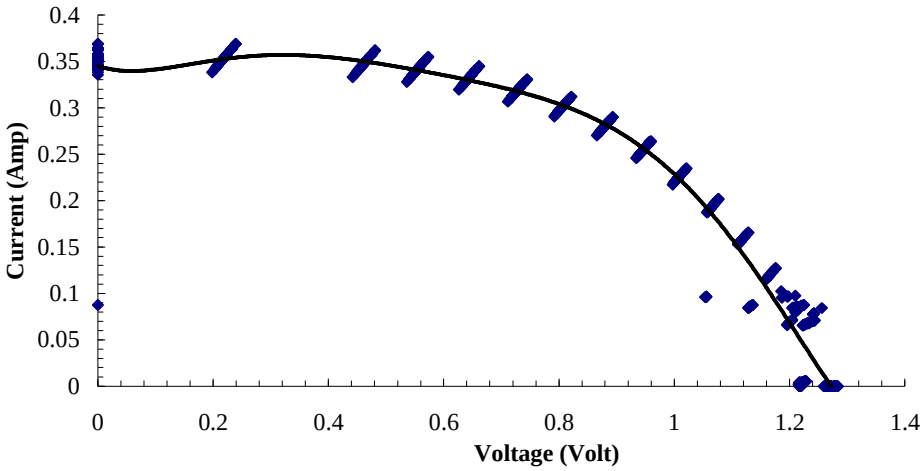

Figure 5.5.1.6 I-V characteristics of **Panel 1** for solar radiation intensity of 200 Wm^{-2}. The ambient room temperature was 20ºC and the radiation incidence angle was 0º.

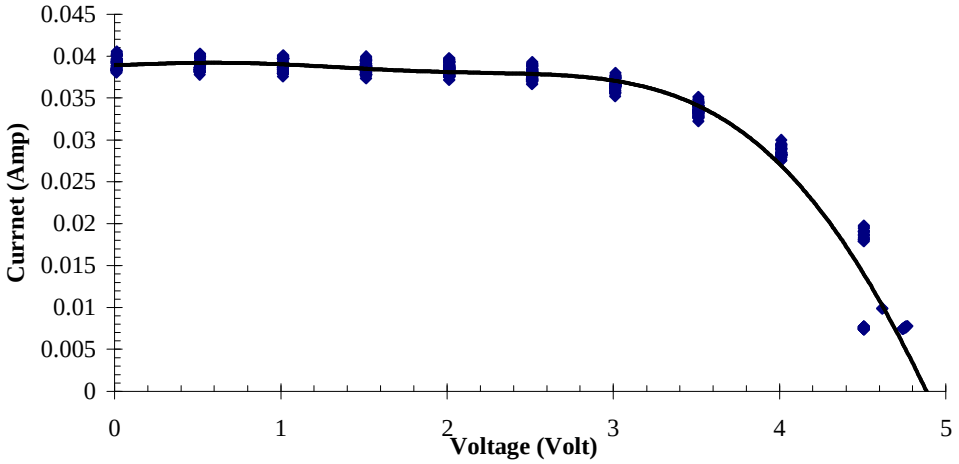

Figure 5.5.1.7 I-V characteristics of **Panel 3** for solar radiation intensity of 200 Wm^{-2}. The ambient room temperature was 20ºC and the radiation incidence angle was 0º.

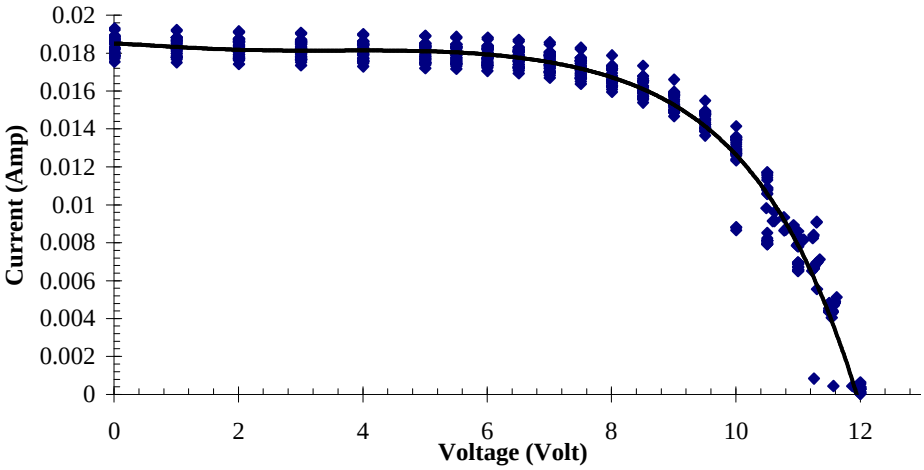

Figure 5.5.1.8 I-V characteristics of **Panel 4** for solar radiation intensity of 200 Wm^{-2}. The ambient room temperature was 20ºC and the radiation incidence angle was 0º.

5.5.2 Effect of Incident Radiation Intensity on the Power Output

The maximum power point increases linearly with the incident solar radiation for each solar panel. The variation of output power with output voltage is shown in figure 5.5.2.1 for **Panel 1** while figure 5.5.2.2 shows the variation of output power to the output voltage for **Panel 2** for a range of incident radiation intensities. From figure 5.5.2.1 and figure 5.5.2.2 it can be seen that output power increased linearly with the incident radiation intensities. For **Panel 1** a 141% increase in power can be seen when the incident solar radiation intensity increased by 250% whereas for **Panel 2**, a 94% increase in power can be seen when the solar radiation increased by 150%. The power variations for both the flat non-concentrating panel and the ACPPVC-50 panel are thus similar. At the short circuit and open circuit conditions the PV produces no power output although the current and voltage attain their maximum values. The maximum power point is shifted towards higher voltage as the solar radiation increases for both the flat non-concentrating panel and the ACPPVC-50.

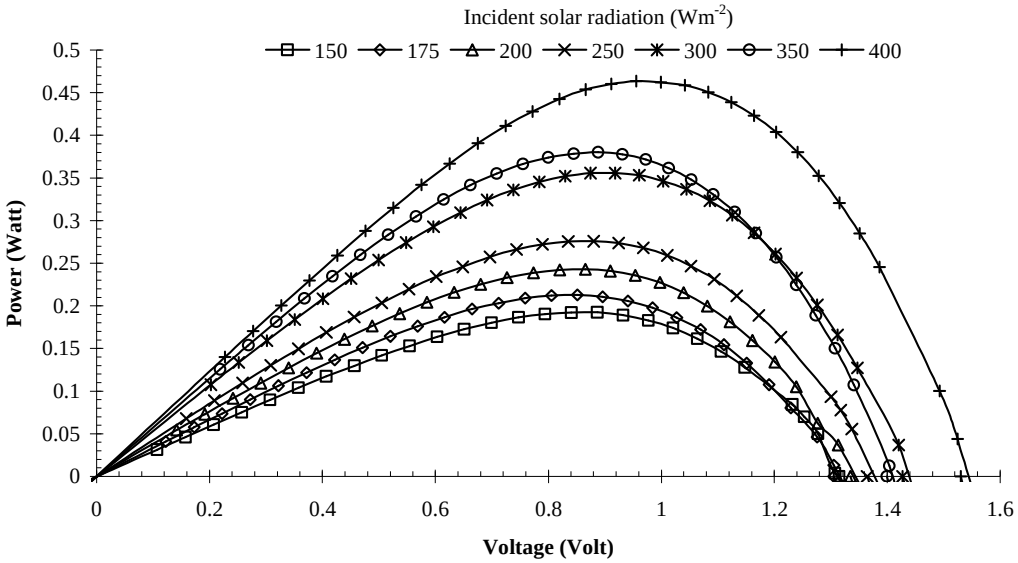

Figure 5.5.2.1 Variation of instantaneous power with sweep voltage for different radiation intensities of **Panel 1**. The ambient room temperature was 20ºC and the radiation incidence angle was perpendicular to the PV surface.

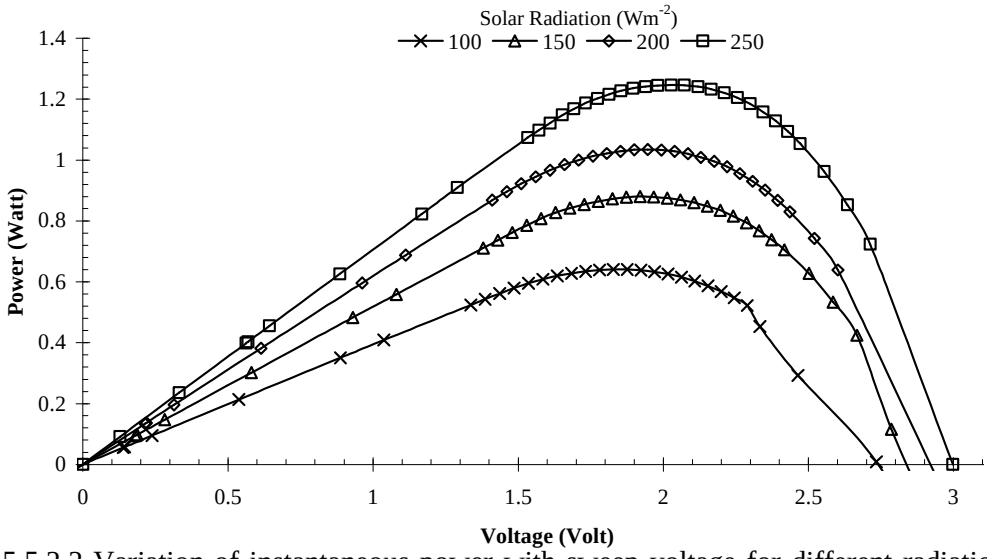

Figure 5.5.2.2 Variation of instantaneous power with sweep voltage for different radiation intensities of **Panel 2**. The ambient room temperature was 20ºC and the radiation incidence angle was perpendicular to the PV surface.

5.5.3 Temperature Dependency of Fill Factor Response for the Three Trough ACPPVC-50 System

The effect of temperature on the ACPPVC-50 performance was investigated by exposing the ACPPVC-50 to continuous solar radiation of 250 Wm^{-2} for 10 hours. Thermocouples were located on the aluminium back plate as shown in figure 5.5.3.1 and temperature measurements were taken at 20 sec intervals. Doors and windows were closed during tests to avoid unwanted air flow that may cause additional heat transfer from the external surfaces.

The variation of temperature with time is presented in figure 5.5.3.2 for radiation incident perpendicular to the PV surface with an intensity of 250 Wm^{-2}. The maximum solar cell temperature of 42.6°C was reached in the central region of the ACPPVC-50 (thermocouple position T_7 as shown in figure 5.5.3.1). A 1.5°C temperature difference occurred between thermocouples in positions T_1 and T_7. The temperatures initially increased exponentially however after 150 minute of exposure (i.e. from 1.30 p.m. onwards) the temperatures vary linearly until it becomes constant. Steady state is attained when the heat input to the PV surface and the heat loss from the external surfaces become equal. The I-V characteristics of the ACPPVC-50 at different solar cell temperatures are shown in figure 5.5.3.3.

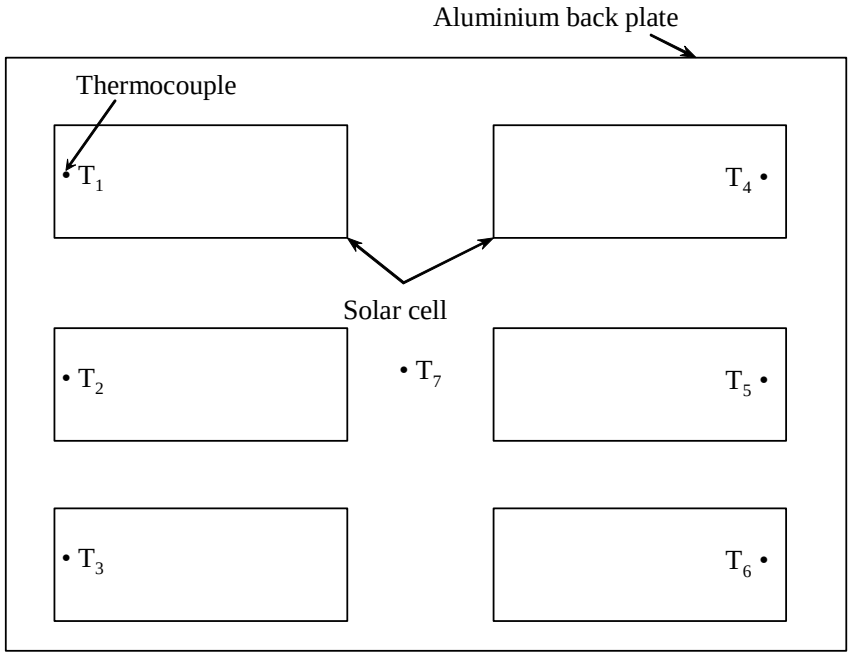

Figure 5.5.3.1 Frontal view of the location of temperature sensors on the rear aluminium back plate of the three trough ACPPVC-50.

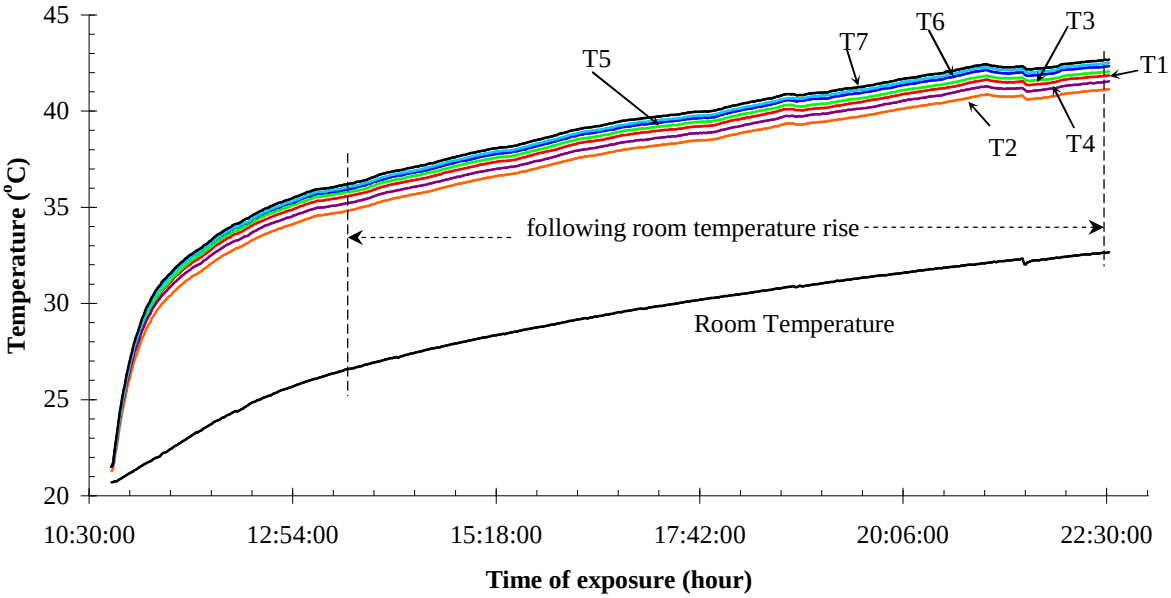

Figure 5.5.3.2 Measured temperatures for the three trough ACPPVC-50 with time of exposure to a constant incident radiation of 250 Wm^{-2}.

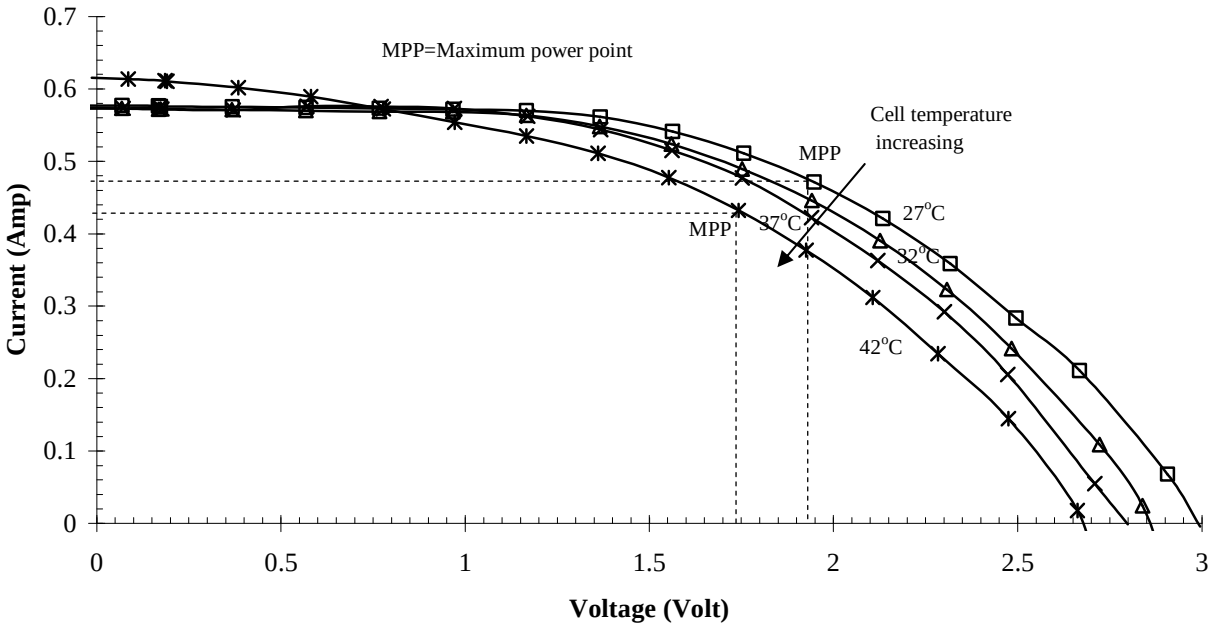

Figure 5.5.3.3 I-V characteristics of the ACPPVC-50 (**Panel 2**) for different solar cell temperatures at solar radiation intensity of 250 Wm^{-2}.

It can be seen from figure 5.5.3.3 that the short circuit current increases by 40 mA and the open circuit voltage decreases by 0.32 V when the solar cell temperature increases by 15ºC, representing a 6.8% reduction in maximum power output generated by the concentrator. The I-V characteristics for different solar cell temperatures for **Panel 4** are shown in figure 5.5.3.4. The solar radiation was 250Wm^{-2} incident perpendicular to the PV surface. It is observed that short circuit current increased by 17.4 mA and open circuit voltage decreased by 1.67 V but the fill factor decreased from 67.5% to 62.56% when solar cell temperature increased from 20ºC to 50ºC.

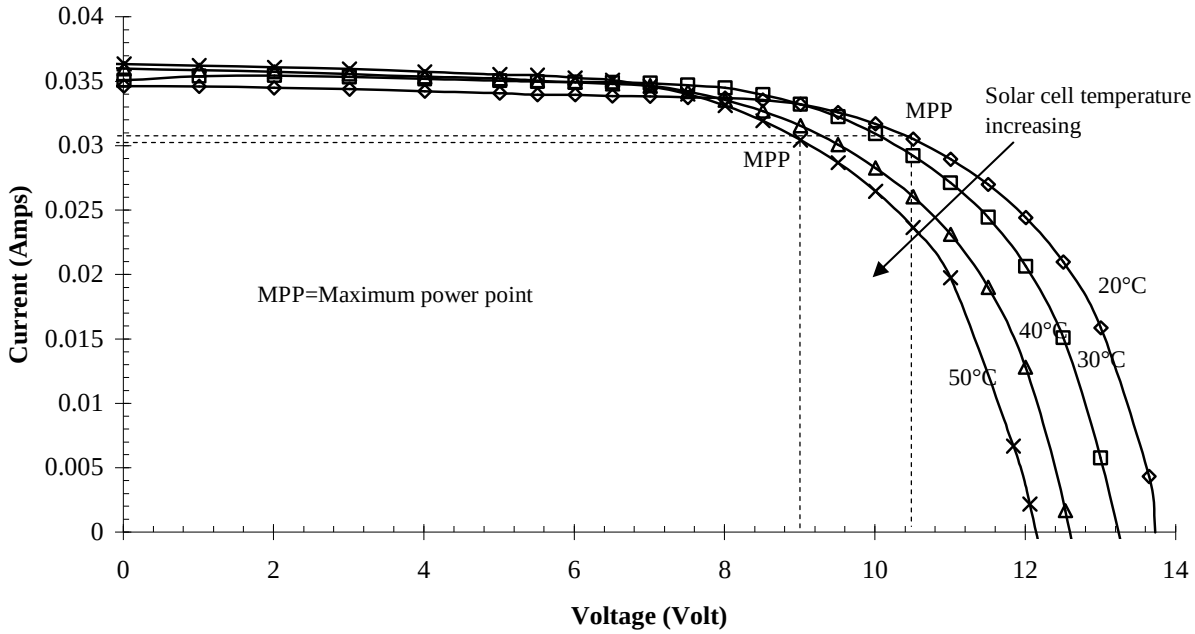

Figure 5.5.3.4 I-V characteristics of the 9-mm wide (**Panel 4**) solar cell non-concentrating flat panel for different solar cell temperatures for a solar radiation intensity of 250 Wm^{-2}.

5.5.4 Variation of Fill Factor with Incident Radiation Intensity and PV Cell Temperature

The fill factor is defined as (Partain, 1995):

$$ff = \frac{I_{\max} V_{\max}}{I_{sc} V_{oc}} \qquad (5.5.4.1)$$

The fill factor for the two panels are (for solar radiation of 300 Wm^{-2}) 47.3% for **Panel 1** and 61% for **Panel 2 (**ACPPVC-50). The fill factor is low for both systems because of power loss in the connecting cables (the Keithley equipment was within a one metre range as shown in figure 5.5.1). The connecting cable has a resistance of 1Ω which implies the power loss of the connecting cable is i^2 Watt (where i is the instantaneous current of the PV system). Since the flat panel has a higher current to voltage ratio compared to the ACPPVC-50 the relative power loss for the flat panel is more significant compared to the ACPPVC-50. The variation in fill factor with incident solar radiation is shown in figure 5.5.4.1 for **Panel 1**. The solar cell temperature was 25ºC and for all incident radiations the solar incidence angle was 0º (perpendicular to the PV surface). The fill factor reaches a maximum value of only 0.5 because of the resistive loss across the connecting cable as can be seen from the corresponding I-V characteristics. Figure 5.5.4.2 shows the variation of fill factor with solar cell temperature for **Panel 3** at an incident radiation intensity of 250 Wm^{-2}. It can be seen from figure 5.5.4.2 that the fill factor decreased by 0.002% for every degree rise in solar cell temperature.

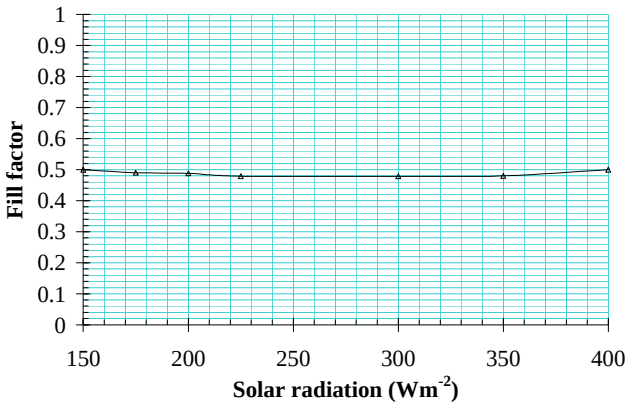

Figure 5.5.4.1 The variation of fill factor for the ACPPVC-50 with incident solar radiation intensities at constant solar cell temperature of 25ºC.

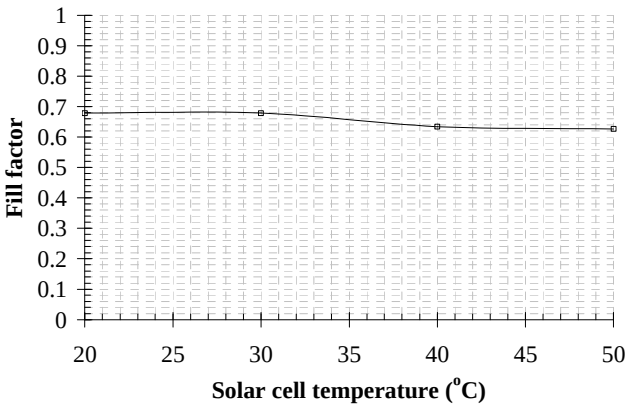

Figure 5.5.4.2 The variation of fill factor with solar cell temperature for **Panel 3** at a solar incident radiation intensity of 250 Wm^{-2}.

5.6 The Effect of Incident Radiation Intensity on Measured Efficiency

The PV system efficiency was calculated as (Partain, 1995):

$$\eta = \frac{P_{\max}}{G_{sol} \times A_{eff}} \tag{5.6.1}$$

or

$$\eta = ff \times \frac{I_{sc} V_{oc}}{G_{sol} \times A_{eff}} \tag{5.6.2}$$

Figure 5.6.1 shows the electrical conversion efficiency of the non-concentrating flat system (**Panel 1**) and the ACPPVC-50 (**Panel 2**) for different incident radiation intensities. The effective area for the flat panel was 3×50×125 mm^2 (**Panel 1**) whereas for the ACPPVC-50 (**Panel 2**) the effective area was 6×100×125 mm^2 and the solar radiation G_{sol} was 200 Wm^{-2}. The solar cell efficiencies are therefore 6.53% for flat **Panel l** and 6.96% for concentrator **Panel 2**. From this it appears that an efficiency improvement of 6.53% was achieved the PV concentrator panel compared to the flat panel.

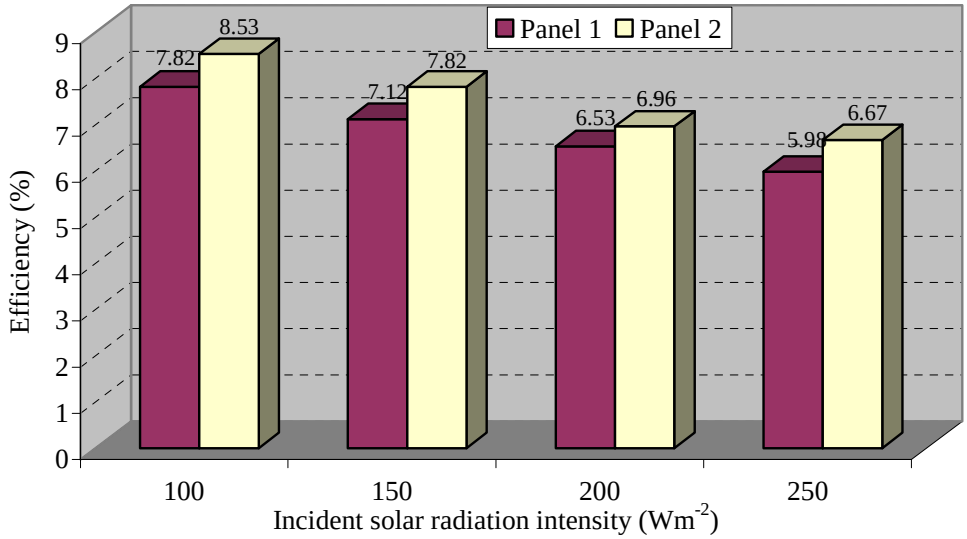

Figure 5.6.1 The variation of electrical conversion efficiency of **Panel 1** and **Panel 2** for different solar incident radiation intensities.

5.7 Variation of Maximum Power Point

It is important to use a PV system at its maximum power point (MPP). The change of maximum power point leads to a change in the efficiency of the system. The ACPPVC-50 with a theoretical concentration of 2.01 effectively increases the solar radiation at the PV surface and thus the short circuit current and open circuit voltage. However the increase in open circuit voltage and short circuit current are not of the same magnitude. The increase in the solar cell temperature due to concentration decreases the open circuit voltage and thus the output power from the PV panel.

The power curves with output voltage for **Panel 1** and **Panel 2** are shown in figure 5.7.1 for solar incident radiation of 250 Wm^{-2}. The short circuit current of the **Panel 2** is increased by 60% whereas the maximum power increased by 117%. This is due to the following reasons:

- **Panel 1** has fill factor of 47.3% whereas **Panel 2** has fill factor of 61%.
- Active PV cell area was half for **Panel 1** compared to **Panel 2** otherwise it was not possible to achieve such solar incident radiation from the solar simulator.

The figure 5.7.2 shows the variation of output power with voltage of **Panel 2** for different solar cell temperatures. The incident radiation intensity was 200 Wm^{-2} perpendicular to the PV surface. For **Panel 2** the maximum power decreased by 18% when the solar cell temperature increased from 27ºC to 42ºC compared to a decrease of 12% of the maximum power when the solar cell temperature increased from 20ºC to 40ºC for **Panel 4**. This power variation with voltage output is shown in figure 5.7.3. For this measurement the solar radiation was 250 Wm^{-2} incident perpendicular to the PV surface. For all the power curves it is obvious that the open circuit voltage drops in a significant manner compared to the increment of short circuit current.

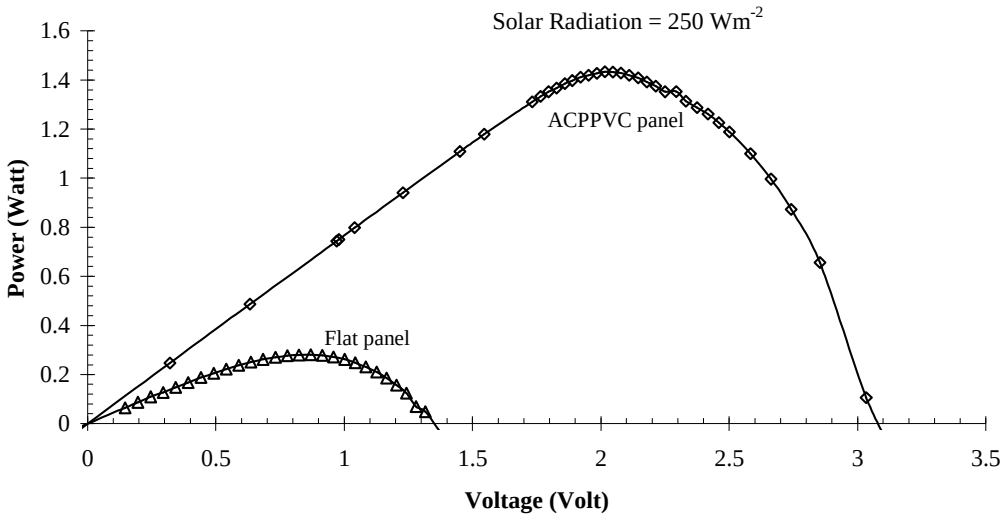

Figure 5.7.1 Variation of power with instantaneous voltage for non-concentrating flat PV panel (**Panel 1**) and ACPPVC-50 system (**Panel 2**) at incident solar radiation intensity of 250 Wm^{-2}.

As detailed in chapter 2, the angle of incidence plays a major role in the optical performance of concentrating systems and their collection efficiency. The power variation with output voltage for the

ACPPVC-50 inclined at different angles is shown in figure 5.7.4. The solar radiation was 250 Wm^{-2} incident perpendicular to the wooden board. At a 10º system inclination angle the maximum power output is achieved from the concentrator, the predicted collection efficiency is 100% and the predicted optical efficiency is at its highest value of 85.5% as calculated in chapter 2. A 10º inclination angle increases the output power by approximately 70% compared to a 0º inclination angle. Although the available power from the panel increased for a 10º inclination angle, the voltage corresponding to the maximum power point (MPP) remains constant.

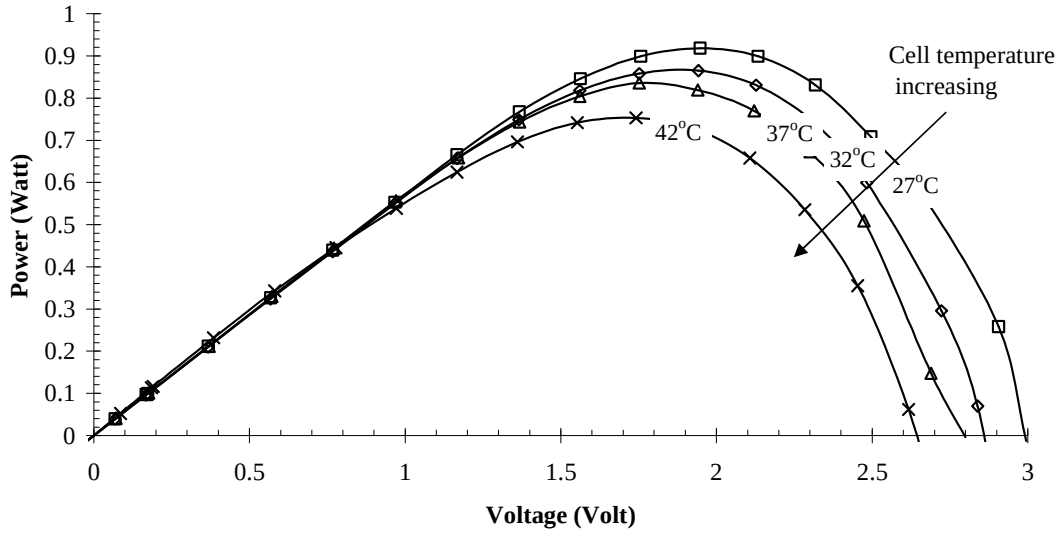

Figure 5.7.2 Variation of power with instantaneous voltage for **Panel 2** (ACPPVC-50) for different PV cell temperatures with radiation intensity of 250 Wm^{-2} incident perpendicular to the PV surface.

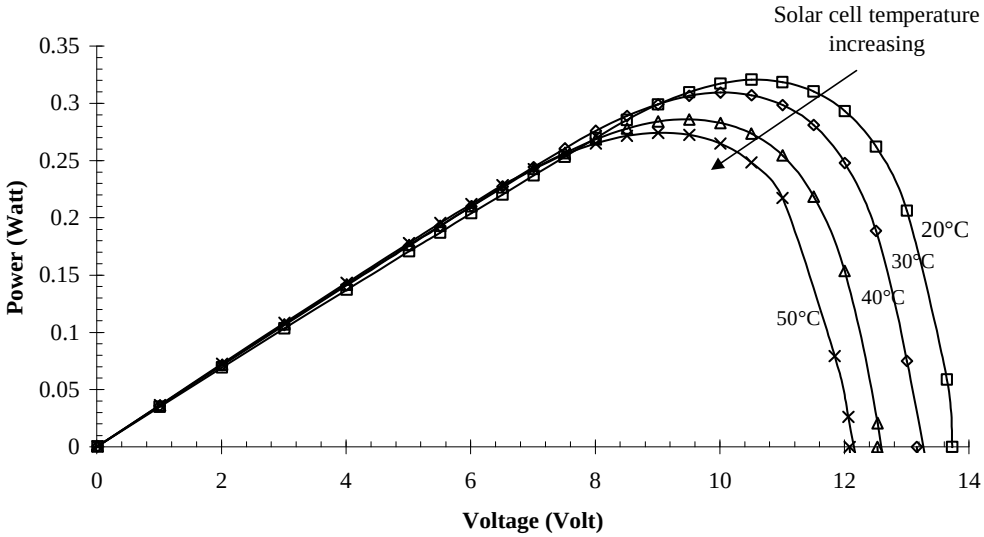

Figure 5.7.3 Variation of power with instantaneous voltage for **Panel 4** for different PV cell temperatures with radiation intensity of 250 Wm^{-2} incident perpendicular to the PV surface.

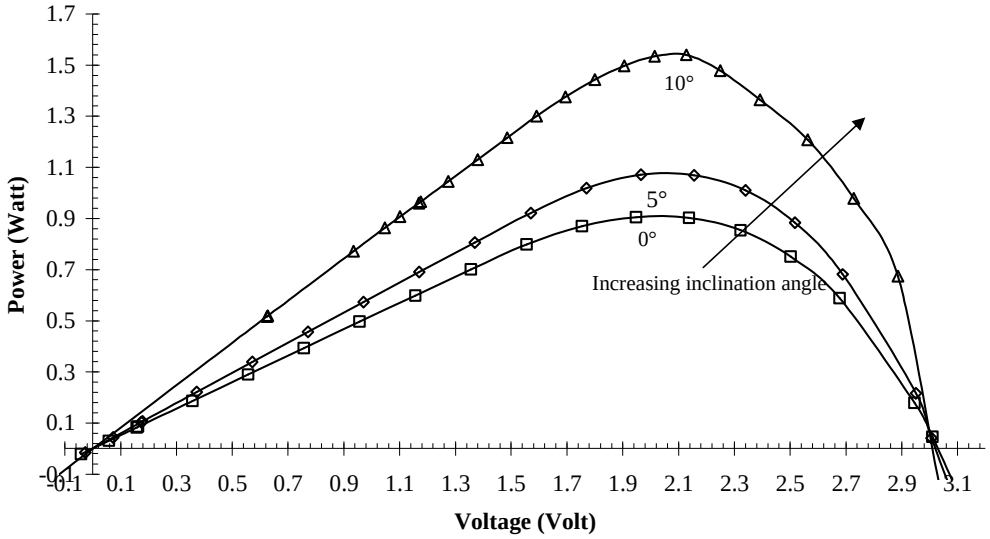

Figure 5.7.4 Variation of output power with output voltage for different inclination angle of the ACPPVC-50 system with solar radiation of 250 Wm^{-2}.

5.8 Conclusions

Four different PV panels were constructed and characterised using a continuous solar simulator. The systems were illuminated with different solar radiation intensities for several hours to determine the temperature effects on the I-V characteristics of the systems. A 94% increase of maximum power is observed for ACPPVC-50 when the incident solar radiation intensity increased by 150% whereas the output power increased by 117% for the ACPPVC-50 compared to the flat panel at same level of intensity. The power output of ACPPVC-50 was measured for 0, 5 and 10º inclination angles. A 10º inclination angle increased the maximum power point by approximately 70% compared to a non-inclined ACPPVC-50. The maximum power output from the ACPPVC-50 is decreased by 1.2% for every °C increase of solar cell temperature but the fill factor decrease by 0.002%$°C^{-1}$. The maximum fill factor achieved was 0.68 for a PV panel using 9-mm wide solar cells.